OXYGEN AND FUEL JET DIFFUSION FLAME STUDIES IN MICROGRAVITY MOTIVATED BY SPACECRAFT OXYGEN STORAGE FIRE SAFETY

P.B. Sunderland and Z.-G. Yuan
National Center for Microgravity Research, Cleveland, OH 44135.

S.S. Krishnan and J.M. Abshire
Department of Mechanical Engineering, IUPUI, Indianapolis, IN 46202.

J.P. Gore
School of Mechanical Engineering, Purdue University, W. Lafayette, IN 47907.

INTRODUCTION

In 1997 there was a fire on the Mir space station that threatened the lives of everyone aboard. The fire involved an oxygen jet leaking from a lithium-perchlorate oxygen generator, as described by Ross [1]. The fire was unusual in that it involved three factors not normally encountered in terrestrial fires: enhanced oxygen, inverse flames (where the oxidizer is surrounded by fuel), and microgravity. Further, there were the following characteristics of these fires that were noted by the astronauts: They produced large amounts of soot and were difficult to extinguish. Therefore it is important to examine the effects of these three factors on laminar diffusion flames and the characteristics of these flames in comparison to normal flames in normal gravity.

Inverse flames have mixture-fraction/temperature/time trajectories for soot processes that are different from those of normal flames. Inverse diffusion flames were reported in 1928 by Burke and Schumann [2]. Sidebotham and Glassman [3], Kaplan and Kailasanath [4] and Blevins et al. [5, 6] have studied inverse diffusion flames. Sunderland et al. [7] used inverse spherical flames to distinguish the effects of convection direction and stoichiometry on soot formation.

OBJECTIVES

Owing to the absence of past work involving flames similar to the Mir fire – namely oxygen-enhanced, inverse gas-jet diffusion flames in microgravity – the objectives of this work are as follows:

1. Observe the effects of enhanced oxygen conditions on laminar jet diffusion flames with ethane fuel.
2. Consider both earth gravity and microgravity.
3. Examine both normal and inverse flames.
4. Compare the measured flame lengths and widths with calibrated predictions of several flame shape models.

This study expands on the work of Hwang and Gore, [8,9] which emphasized radiative emissions from oxygen-enhanced inverse flames in earth gravity, and Sunderland et al., [10] which emphasized the shapes of normal and inverse oxygen-enhanced gas-jet diffusion flames in microgravity.

MICROGRAVITY EXPERIMENTS

The present experiments involve ethane reacting with oxygen/nitrogen mixtures with oxygen mole fractions of 0.21, 0.3, 0.5 and 1. The flames were attached to a round stainless-steel burner with an inside diameter of 5.5 mm and a knife-edge tip. The burner tube was straight and unobstructed for a length of 25 cm upstream of its tip. The ambient gas was quiescent at 0.98 bar and 298 K and was contained in a cylindrical windowed pressure vessel.

The earth-gravity tests were conducted with the burner gas injecting vertically upward. The microgravity tests were performed in the NASA Glenn 2.2-second drop tower. Details of the rig were reported in Sunderland et al. [10]. The flames were imaged using a color CCD camera with a 25 mm manual-iris lens, recorded on analog color video and analyzed subsequently.

The lengths and widths of the microgravity flames were measured from the video recordings. Where blue contours were not obscured by soot, flame sheet lengths were measured from the burner tip to the peak of blue intensity. Where contours were obscured, flame luminosity lengths were measured from the burner tip to the end of the yellow region. Flame sheet widths were not obscured by soot for any flame and were defined as the width of the contour of peak blue intensity at its widest. Repeatability of the flame length and width measurements was ±5%.

Four oxidizer compositions each for normal and inverse flames in earth gravity and microgravity i.e., a total of 16 flames, were studied. The burner gas velocity for the inverse flames was held constant at 866 mm/s. The ethane flowrates for the normal flames were chosen to match the heat release rates of the corresponding inverse flames, such rates being determined using a lower heating value of ethane of 47 KJ/g. This choice of flowrates yielded a relatively small variation in flame sheet length for all flames. The present Reynolds numbers confirm that the discharge conditions were laminar.

FLAME SHAPE PREDICTIONS – APPROACH

Descriptions of the different models used in the present study are described in Sunderland et al. [10]. One of the models used, the Roper model following Roper [11] and its results are described in better detail here and in Sunderland et al. [10]. A Matlab code was developed to predict the flame shape using the governing equation for the conserved scalar, C which is a non-dimensionalized mixture fraction. Romberg integration and Newton-Raphson iterative methods were used to solve for the flame shape for a given C_{st} which defined the flame sheet. A uniform velocity profile of magnitude equal to the burner exit velocity is assumed at all axial locations. The resulting flame shape was obtained in terms of r and z coordinates. A plot of the flame shape curve was obtained in Matlab.

The flame images from the experimental results in JPG format and the flame shape curve predicted by the Roper model from Matlab were copied into AutoCAD. The CCD image used square pixels. The Matlab-generated curve was spline-fitted in AutoCAD after magnification to preserve the shape. The scales of a ruler image from the flame image and the scale of the flame shape curves were matched in AutoCAD.

RECENT RESULTS

Only the most recent results are shown here. Other results have been reported in Sunderland et al. [10, 12]. Figures 1 (a) and 1(b) show still color images of eight microgravity normal and inverse flames respectively. The Roper model predictions are shown overlayed on the images and show excellent agreement with the experimental flame shapes. The shift in the prediction for

the first two normal flames in figure 1(a) is due to the neglect of axial diffusion effects which become predominant in these flames. In these images soot is identified by white, yellow, or orange coloration, and stoichiometric flame sheets are identified by blue emissions.

In general, the earth-gravity flames were reported earlier as much narrower than their microgravity counterparts owing to buoyantly induced entrainment [10]. The normal flames have undiluted C_2H_6 flowing from the burner. With the exception of microgravity normal flame 21, which is blue, all these flames contain soot, which first appears inside the flame sheet near the burner. Increasing oxidizer concentration yields brighter flames, as revealed by the images and their relative exposures. The normal microgravity flames were seen to increase in length and width and to decrease in brightness throughout the 2.2 s tests. Large soot aggregates, on the order of 1 mm, are seen being emitted from microgravity flames 30 and 50.

Figure 1(b) shows color images of the present inverse flames in microgravity. All these flames contain soot, which forms and resides on the fuel side of the flame sheet and which is emitted into the ambient ethane gas. Increasing oxidizer concentration yields brighter flames, as revealed by the images and their relative exposures. Unusual variations in blue intensity in the inverse flames, also noted in Hwang and Gore [8], complicate the precise identification of the stoichiometric contours of these flames.

The present microgravity inverse flames have annular soot layers which start near the burner tip, expand with axial distance until just below the stoichiometric flame tip, and contract above this. Most of the soot formation in these flames occurs on the rich side of the flame near the stoichiometric flame sheet. The newly-formed soot is then driven radially outward by thermophoresis and volumetric expansion caused by heat release overcoming the inward flow caused by the action of viscosity and resulting in a soot annulus. The contraction of the annulus above the flame is attributed to radial inflow in a region with significantly lower thermophoresis and volumetric expansion. Finally, in figure 1(b), the agreement with the Roper prediction is seen to be excellent in these flames. The area near the burner tip is not shown due to the invalidity of the far-field assumption.

Figure 2 shows the quantitative comparisons of inverse flame lengths and widths using the Roper and Spalding models. The inverse diffusion flame widths are predicted better by the Roper model. More work is needed to understand the models and how they work for the different cases. A detailed computational model is planned as part of future work.

CONCLUSIONS

Ethane fueled laminar gas-jet diffusion flames were observed, emphasizing the effects of oxygen enhancement, gravity, and inverse burning on flame appearance and sooting behavior. The major findings were:

1. Oxygen-enhanced conditions caused increases in soot production, soot emission, and luminosity for both normal and inverse flames. This attests to the increased fire hazards associated with oxygen-enhanced combustion.
2. Microgravity flame shape predictions with Roper and Spalding models were considered. The shapes captured by the Roper model closely agree with the experimental photos. However, a proper evaluation can be accomplished only by additional measurements such as peak temperature and location of the stoichiometric mixture fraction contours and a more detailed computational model.

ACKNOWLEDGEMENT

This work was supported by NASA's Office of Biological and Physical Processes under the management of Merrill King. Alisha Vachhani assisted with the microgravity experiments. The assistance of David Urban was invaluable. We acknowledge helpful discussions with Linda Blevins in the early part of this work.

REFERENCES

[1] H.D. Ross, in: H.D. Ross (Ed.), Microgravity Combustion, Academic Press, San Diego, 2001, pp. 1-34.
[2] S.P. Burke, T.E.W. Schumann, Ind. Eng. Chem. 20 (10) (1928) 998-1004.
[3] C G.W. Sidebotham, I. Glassman, Combust. Flame 90 (1992) 269-283.
[4] C.R. Kaplan, K. Kailasanath, Combust. Flame 124 (2001) 275-294.
[5] L.G. Blevins, R.A. Fletcher, B.A. Benner, E.B. Steel, G.W. Mulholland, Proceedings of the Combustion Institute, Vol. 28, The Combustion Institute, Pittsburgh, 2002, p. 29.
[6] L.G. Blevins, N.Y.C. Yang, M.A. Mikofski, G.W. Mulholland and R.W. Davis, AIAA 41st Aerospace Sciences Meeting and Exhibit, Reno, January 2003.
[7] P.B. Sunderland, R.L. Axelbaum, D.L. Urban, B.H. Chao, S. Liu, Combust. Flame, 132 (2003) 25-33.
[8] S.S. Hwang, J.P. Gore, KSME Intl. J. 16 (9) (2002) 1156-1165.
[9] S.S. Hwang, J.P. Gore, Proc. Inst. Mech. Eng. A - J. Power Energy, 216 (2002) 379-386.
[10] P.B. Sunderland, S.S. Krishnan, and J.P. Gore, AIAA 41st Aerospace Sciences Meeting and Exhibit, Reno, January 2003.
[11] F.G. Roper, Combust. Flame 29 (1977) 219-226.
[12] P.B. Sunderland, S.S. Krishnan, and J.P. Gore, Combust. Flame, submitted (2003).

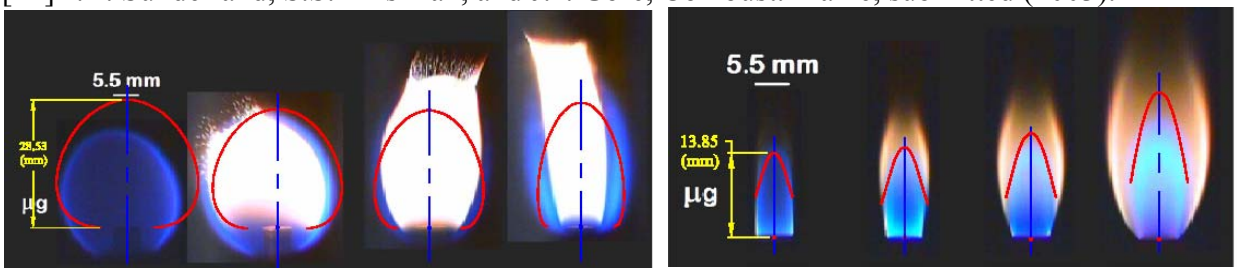

Figure 1. Comparisons between Roper model predictions and microgravity experimental results – (a) Normal and (b) Inverse Diffusion Flames (ethane with 21, 30, 50 and 100 % oxygen) (NOTE: Figure 1(b) is not to the same scale as Figure 1(a)).

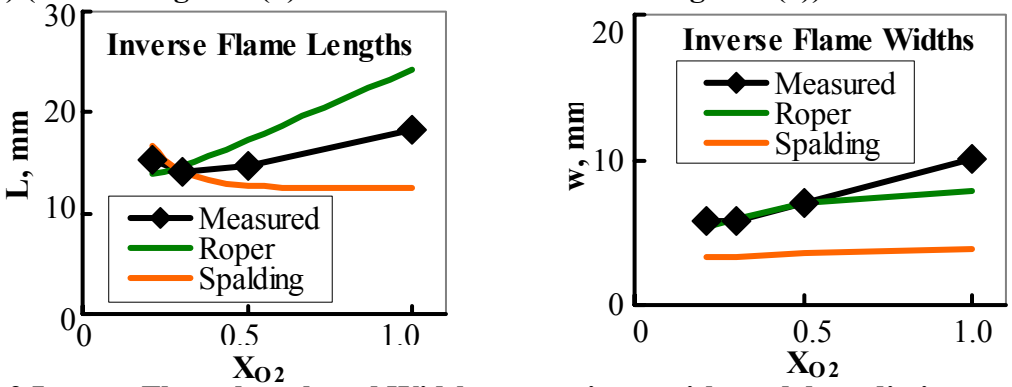

Figure 2 Inverse Flame length and Width comparisons with model predictions.